Active Site Hydrophobicity Is Critical to the Bioluminescence Activity of *Vibrio harveyi* Luciferase†

Chi-Hui Li and Shiao-Chun Tu*

Department of Biology and Biochemistry, University of Houston, Houston, Texas 77204-5001

Received May 19, 2005; Revised Manuscript Received August 1, 2005

ABSTRACT: *Vibrio harveyi* luciferase is an $\alpha\beta$ heterodimer containing a single active site, proposed earlier to be at a cleft in the α subunit. In this work, six conserved phenylalanine residues at this proposed active site were subjected to site-directed mutations to investigate their possible functional roles and to delineate the makeup of luciferase active site. After initial screening of Phe → Ala mutants, αF46, αF49, αF114, and αF117 were chosen for additional mutations to Asp, Ser, and Tyr. Comparisons of the general kinetic properties of wild-type and mutated luciferases indicated that the hydrophobic nature of αF46, αF49, αF114, and αF117 was important to luciferase V_{max} and V_{max}/K_m, which were reduced by 3−5 orders of magnitude for the Phe → Asp mutants. Both αF46 and αF117 also appeared to be involved in the binding of reduced flavin substrate. Additional studies on the stability and yield of the 4a-hydroperoxyflavin intermediate II and measurements of decanal substrate oxidation by αF46D, αF49D, αF114D, and αF117D revealed that their marked reductions in the overall quantum yield ($\phi_\circ$) were a consequence of diminished yields of luciferase intermediates and, with the exception of αF114D, emission quantum yield of the excited emitter due to the replacement of the hydrophobic Phe by the anionic Asp. The locations of these four critical Phe residues in relation to other essential and/or hydrophobic residues are depicted in a refined map of the active site. Functional implications of these residues are discussed.

In the bioluminescence reaction catalyzed by bacterial luciferase, a flavin-dependent monooxygenase, reduced riboflavin 5′-phosphate ($FMNH_2$)[1] and a long-chain aliphatic aldehyde are oxidized by molecular oxygen to produce FMN, H_2O, aliphatic carboxylic acid, and visible light with an overall quantum yield ($\phi_\circ$) of about 0.12. It is intriguing that bacterial luciferase is unique among all known flavin-dependent monooxygenases in catalyzing a light-emitting reaction. The proposed minimal mechanism of the luciferase bioluminescence reaction is depicted in Scheme 1 (*1*, *2*). The luciferase-bound N1-deprotonated $FMNH^-$ (intermediate I) reacts with molecular oxygen to generate a 4a-hydroperoxy−FMNH intermediate (HF-4a-OOH or II), which either undergoes a dark decay to produce FMN and H_2O_2 in the absence of aldehyde or reacts with aldehyde to form 4a-peroxyhemiacetal−FMNH (HF-4a-OOCH(OH)R or III). Intermediate III undergoes a still poorly understood reaction to generate carboxylic acid and an excited-state species 4a-hydroxy−FMNH* (HF-4a-OH* or IV*). The relaxation of IV* to the ground state is accompanied by light emission. Finally, the decay of the ground-state IV produces FMN and water and regenerates the free luciferase.

Bacterial luciferase is a heterodimer having molecular masses of 40 and 37 kDa for the α and β subunits, respectively (*3*). The crystal structure of the *Vibrio harveyi* luciferase has been solved at the resolutions of 2.4 and 1.5 Å in the absence of any bound substrate or specific inhibitor (*4*, *5*). Hence, the exact location and atomic structure of the luciferase active site have thus far not been directly determined. The α and β chains display 32% sequence identity, both assume a $(\beta/\alpha)_8$ barrel structure, and the α carbon main chain of these two subunits are nearly superimposable (*4*). Yet, interestingly, there is only one binding site for each of the $FMNH_2$ (*6*) and aliphatic aldehyde (*7*) substrates. *V. harveyi* luciferase also has a weak aldehyde inhibitor site, which is independent from the aldehyde substrate site but overlaps with the $FMNH_2$ site. Contrary to the rapid equilibrium binding of the aldehyde and $FMNH_2$ substrates, the binding and release of aldehyde by this inhibitor site are both much slower (*7*). Therefore, inhibition is observed only when a high level of aldehyde is added to luciferase prior to $FMNH_2$.

In lieu of an atomic structure, a pocket near the C-terminal end of the β barrel in the α subunit of *V. harveyi* luciferase has been proposed to be the general location of the active site by comparisons with the active sites of some other $(\beta/\alpha)_8$ barrel enzymes (*4*, *5*). This proposed active site pocket is supported by other considerations and findings. The original crystal structure of luciferase has a bound phosphate directly interacting with αR107 next to this pocket (*4*). This phosphate site was proposed to be the same binding site for the phosphate in $FMNH_2$ (*4*), and a later mutagenesis study (*8*) provides experiment support for this interpretation. A *cis*

† Supported by grants GM25953 from the National Institutes of Health and E-1030 from The Robert A. Welch Foundation.

* Corresponding author: Dr. Shiao-Chun Tu, Department of Biology and Biochemistry, University of Houston, Houston, TX 77204-5001. Phone, 713-743-8359; fax, 713-743-8351; e-mail, dtu@uh.edu.

[1] [1]Abbreviations: $FMNH_2$, reduced riboflavin 5′-phosphate; FMN, oxidized riboflavin 5′-phosphate; q, quantum; $\phi_\circ$, overall quantum yield of the luciferase reaction; ϕ_{IV^*}, emission quantum yield of the excited luciferase emitter; k_D, the rate constant for the dark decay of intermediate II in the absence of aldehyde.

10.1021/bi050935y CCC: $30.25
Published on Web 09/09/2005

Scheme 1

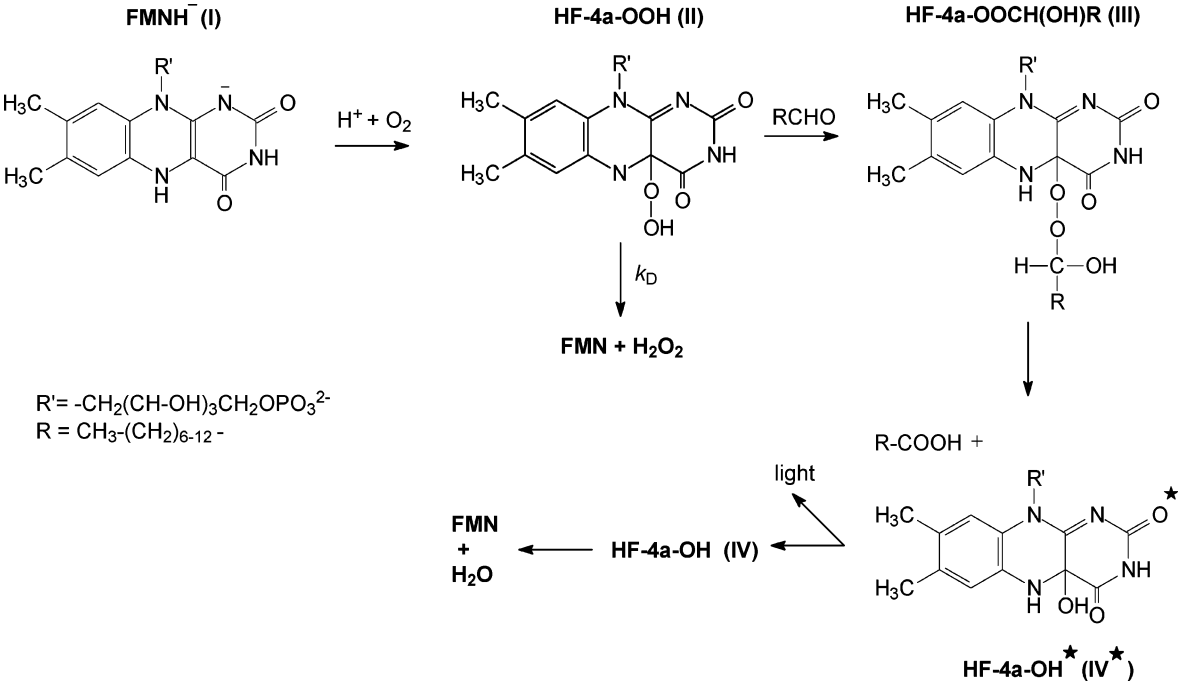

peptide linkage was found between αA74 and αA75 bordering this pocket (*5*). The existence of the rare nonprolyl *cis* bond is generally considered as suggestive evidence for its involvement in ligand binding or catalysis. A computational model of the active site is consistent with and further supports the proposed general location of the active site (*9*). On the basis of this computationally modeled active site, mutations of selected residues were found to affect luciferase activity or the color of the bioluminescence (*10, 11*).

A key structural difference between the α and *β* subunits is a 29-residue loop from α258 to α286 that does not exist in the *β* subunit. This loop is structurally disordered; the segments of α272−α288 and α262−α290 are, respectively, not resolved in the 2.4 and 1.5 Å crystal structures of luciferase (*4, 5*). This mobile loop is located right next to the opening of the proposed active site pocket and has been postulated to be important to the gating of the active site by, while in a closed configuration, shielding the intermediates during the catalysis (*3*). This postulate is supported by site-directed mutagenesis studies carried out in our laboratory, which show that the torsional flexibility of the αG275 and the hydrophobic and bulky nature of the αF261 within this loop are both essential to the luciferase light-emitting activity (*12*).

The above-mentioned mutational study shows that the V_{max} (i.e., the maximal bioluminescence intensity) of luciferase can be reduced about 5 orders of magnitude by the αF261D mutation. In comparison with the mutational effects on the yields of various intermediates, one major cause for the much reduced luciferase activity is the drastically diminished emission quantum yield of the excited emitter IV* (ϕ_{IV*}) when the hydrophobic αF261 is replaced by the anionic aspartyl residue (*12*). Recently, we found that the fluorescence quantum yield of 5-decyl-4a,5-dihydroriboflavin-5′-phosphate, a model for the luciferase emitter IV*, is increased 3 orders of magnitude by binding to luciferase active site (*13*). These findings indicate the hydrophobicity of the luciferase active site is essential to a high ϕ_{IV*} and, hence, the overall $\phi_{\circ}$. The present study was carried out to further test this working hypothesis by identifying additional conserved hydrophobic residues in the proposed active site pocket and examine the mutational effects of selected residues on the bioluminescence activities and intermediate yields of the mutant luciferases. The results allowed us to further establish the importance of the hydrophobicity of luciferase active site to the luminescence activity, identify additional critical phenylalanyl residues, and better define the boundary of the luciferase active site.

EXPERIMENTAL PROCEDURES

Materials. Site directed mutagenesis kit and competent cells *Escherichia coli* JM101 were from Strategene. Oligonucleotide primers were products of MWG Biotech. FMN, dodecanol, decanal, and sodium hydrosulfite were purchased from Sigma. DEAE-cellulose DE52 and DEAE-sepharose were from Whatman and Pharmacia, respectively. Wizard SV Plus Miniprep kits and dithiothreitol were from Promega. All decanal solutions were prepared in absolute ethanol. The 50 mM standard phosphate (Pi) buffer was at pH 7.0 with molar fraction of 0.39 for sodium monobase and 0.61 for potassium dibase in deionized water.

Luciferase Mutants. *V. harveyi luxAB* genes encoding luciferase *αβ* heterodimer were harbored in the pUC19 vector. Stratagene Quickchange Site-Directed Mutagenesis kit was used to perform mutation in *luxA*. The codon TTC of αF46 was modified to GCC, GAC, TCC, and TAC for alanine (αF46A), aspartate (αF46D,), serine (αF46S), and tyrosine (αF46Y). The codon TTT for αF49, αF114, and αF117 was modified to GCT, GAT, TCT, and TAT for alanine (αF49A, αF114A, αF117A), aspartate (αF49D, αF114D, and αF117D), serine (αF49S, αF114S, and αF117S), and tyrosine (αF49Y, αF114Y, and αF117Y). Protocols along with the kit were followed to obtain mutants. Those PCR-based mutageneses were confirmed by sequencing by

the Lone Star Lab. Each mutant was then transformed into *E. coli* JM101 competent cells according to the protocol included in the kit from Stratagene.

Luciferase Purification and Activity Assays. Each luciferase variant was overexpressed at 37 °C for 16∼20 h till the OD_{600} reached at least 4 and purified, according to the protocol previously described (*14*), from host strain *E. coli* JM101 to ≥85% homogeneity based on patterns of sodium dodecyl sulfate−polyacrylamide gel electrophoresis. The luciferase activity was determined in 50 mM standard Pi buffer (pH 7.0) at 23 °C using a calibrated photometer with FMN reduced by dithionite or Cu−I as previously described (*7*, *15*). After the onset of the reaction, the autoxidation of excess free $FMNH_2$ is much faster than the luciferase-catalyzed oxidation of the bound $FMNH_2$. Hence, the luciferase light emission time course in activity assay is that from a single-turnover reaction. The bioluminescence quickly reached a peak within a second and then decayed exponentially. The activity (v) of luciferase was directly determined as the peak intensity of the bioluminescence in q/s. Michaelis constants for decanal (K_{mA}) and $FMNH_2$ (K_{mF}) and V_{max} were determined from double-reciprocal plots of results obtained from substrate titration experiments. For comparisons of V_{max} of various species of luciferases, enzyme concentrations were normalized to eliminate differences in enzyme sample purity.

Stability of 4a-Hydroperoxy−FMNH Intermediate II. Intermediate II was formed by the addition of a slight excess amount of sodium dithionite to a 50 mM Pi buffer containing 50 μM FMN and a desired species of luciferase followed by gentle mixing under aerobic conditions. The initial bleaching of the yellow sample color indicated the reduction of FMN. After mixing for seconds, the solution changed from clear back to yellow, indicating the exhaustion of dithionite and the re-formation of FMN from free $FMNH_2$. By this time, the luciferase-bound $FMNH_2$ also underwent oxidation to become intermediate II. After different times of incubation at 23 or 4 °C, 100-μL aliquots were withdrawn for activity assays at 23 °C. A parallel experiment was performed with 75 μM dodecanol included in the luciferase−FMN solution to stabilize the intermediate II (*16*). The rate constant for the dark decay of intermediate II (k_D) was determined by a semilogarithmic plot of $I/I_\circ$ versus time in which $I_\circ$ and I are, respectively, the bioluminescence activities detected at time zero when the intermediate II was first formed and after a given period of time of standing after the II formation.

Stopped-Flow Spectrophotometry. A 50 mM Pi solution containing 50 μM FMN (or 200 μM FMN for the αF117D-catalyzed reaction) and 10 mM EDTA was made anaerobic by repeated evacuation and equilibration with nitrogen in an airtight flask. FMN was reduced by long wavelength UV, and the bleached $FMNH_2$ solution was then withdrawn into an airtight stopped-flow syringe. A separate 135 μM luciferase solution was prepared in an air-saturated 50 mM Pi buffer in another syringe. The luciferase-catalyzed oxidation of $FMNH_2$ was initiated by mixing 120 μL of solution from each syringe by using an Olis RSM 1000 stopped-flow spectrophotometer at 23 °C. The absorbance changes at 382 and 445 nm over time were collected after the mixing and were normalized as $\Delta A/\Delta A_\infty$, where ΔA and ΔA_∞ are the increases of absorbance from time zero immediately after mixing to, respectively, a given time after the mixing and upon the completion of the reaction. Kinetics and absorbance changes during the autoxidation of $FMNH_2$ were similarly determined by mixing the $FMNH_2$ solution with an air-saturated phosphate buffer without luciferase.

Aldehyde Consumption. A decanal standard curve based on light intensities obtained in luciferase assays at different decanal concentrations was first constructed as described before (*14*). A 1-mL 50 mM Pi buffer solution containing a specified level of $FMNH_2$ (prepared by the Cu−I reduction method) was injected into an equal volume of buffer containing 1 μM decanal and 20 μM wild-type or mutant luciferase. After the completion of the bioluminescence reaction, 20 μL aliquots of the sample were withdrawn and used as aldehyde sources for the determination of the amounts of remaining decanal. Control sample was prepared similarly but with the Cu−I-reduced $FMNH_2$ completely reoxidized before injection to the luciferase/decanal solution.

RESULTS

Site-Directed Mutagenesis. To investigate the relationship between luciferase active site hydrophobicity and bioluminescence activity, a number of phenylalanyl residues were targeted for mutation on the basis of two criteria, namely, presence at or within the boundary of the proposed active pocket and conservation in primary sequences of luciferases from *V. harveyi, Kryptophanaron alfredi, Vibrio fischeri, Photobacterium phosphoreum, Photobacterium. leiognathi, and Xenohabdus luminescens* (*17*). Six phenylalanyl residues (namely αF6, αF46, αF49, αF114, αF117, and αF327) were so identified, and each was first mutated to alanine. Plasmids harboring these mutated luciferase genes were transformed into *E. coli* JM101 host cells. Markedly reduced in vivo bioluminescence (triggered by the addition of decanal) was observed with cells expressing the αF46A, αF49A αF114A, and αF117A mutants, but little changes in bioluminescence were observed with the other two mutants. Therefore, for subsequent studies, the residues αF46, αF49 αF114, and αF117 were each mutated to three additional types of residues (i.e., Asp, Ser, and Tyr), and all luciferase variants derived from these mutations were purified and subjected to detailed characterizations.

General Kinetics Properties of Luciferase Variants. The general kinetic properties of all 16 luciferase mutants and that of the wild-type luciferase were determined and summarized in Table 1. In comparison with the wild-type luciferase, no significant change in the Michaelis constant for decanal (K_{mA}) was detected for αF46A, whereas all other luciferase variants showed significantly but not drastically increased values up to a 6-fold increase for αF49Y. The effects of mutations on the K_{mF} were more variable. In comparison with the native luciferase, relatively little changes in K_{mF} values were observed for the four types of mutation of residue αF49 or αF114. For αF46 and αF117, mutational effects on the K_{mF} values ranged from marked increases for the mutation to the anionic Asp (i.e., 247- and 87-fold increases for αF46D and αF117D, respectively) to less pronounced increases for their neutral Ser and Ala mutations, to a slight reduction in value for the mutation to the hydrophobic Tyr. The V_{max} values for all luciferase variants were significantly reduced. For each of αF46, αF49, αF114, and αF117, the most pronounced (ranging from 3 to 5 orders

Table 1: General Kinetic Properties[a] of Wild-Type Luciferase and Variants

enzyme	K_{mA} (μM)	K_{mF} (μM)	relative V_{max}	relative V_{max}/K_{mF}
wild-type	1.6	0.6	1	1
αF46D	3.2	148	3.6×10^{-3}	8.0×10^{-4}
αF46S	2.6	4.3	9.3×10^{-2}	1.4×10^{-2}
αF46A	1.3	12.3	2.2×10^{-2}	1.2×10^{-2}
αF46Y	2.4	0.3	1.5×10^{-1}	2.9×10^{-1}
αF49D	3.0	1.3	3.2×10^{-5}	1.6×10^{-5}
αF49S	3.3	0.7	3.4×10^{-4}	3.3×10^{-4}
αF49A	3.0	2.7	$2.3 \times 10-4$	5.4×10^{-5}
αF49Y	10.1	0.6	2.9×10^{-2}	2.8×10^{-2}
αF114D	7.3	1.0	4.2×10^{-3}	2.7×10^{-3}
αF114S	8.3	0.2	6.7×10^{-2}	2.7×10^{-1}
αF114A	9.3	0.3	7.8×10^{-2}	1.6×10^{-1}
αF114Y	2.7	0.3	2.5×10^{-1}	5.5×10^{-1}
αF117D	3.1	52	8.2×10^{-4}	1.0×10^{-5}
αF117S	2.4	1.3	2.6×10^{-2}	1.4×10^{-2}
αF117A	3.0	1.5	2.7×10^{-2}	1.2×10^{-2}
αF117Y	5.1	0.3	4.3×10^{-1}	9.9×10^{-1}

[a] K_{mA} and K_{mF} are Michaelis constants for decanal and $FMNH_2$, respectively.

of magnitude) reductions were always associated with the Phe → Asp mutation, the least activity decreases were always for the Phe → Tyr mutation, and intermediate effects were observed for the mutations to Ser and Ala. Since mutations gave rise to more variable K_{mF} than K_{mA} values, only the V_{max}/K_{mF} values are shown in Table 1 for all the mutants for comparisons with that of the wild-type luciferase. Qualitatively similar to the mutational effects on V_{max}, the αF46, αF49, αF114, and αF117 showed the most pronounced reductions in V_{max}/K_{mF} for the Phe → Asp mutation, the least activity decreases for the Phe → Tyr mutation, and intermediate decreases for mutations to Ser and Ala.

While the wild-type luciferase and the αF46D, αF49D, and αF117D variants all showed single-exponential light decays in the single-turnover bioluminescence reaction (with respective k at 13.1, 5.6, 0.8, and 14.0 min^{-1}), αF114D exhibited a double-exponential decay time course (k_1 and k_2 at 30 and 0.4 min^{-1}, respectively).

Quantum Yield and Intermediate II Dark Decay. Since the four Phe → Asp mutants showed the most pronounced reductions in V_{max} and V_{max}/K_{mF}, they were selected for all subsequent characterizations with results summarized in Table 2. The overall quantum yields ($\phi_\circ$) of the native and mutated luciferases were determined by measuring their total quantum outputs over the complete time course of emission. All four Phe → Asp luciferase variants were associated with much reduced $\phi_\circ$, about 2−4 orders of magnitude lower than that of the wild-type enzyme. The rate constants of intermediate II dark decay (k_D) in the absence of aldehyde substrate were determined at 23 and 4 °C, in the absence and presence of 75 μM dodecanol as a stabilizing agent (*16*). At 23 °C in the absence of dodecanol, αF46D, αF49D, αF114D, and αF117D produced slightly more labile intermediate II species, having 1.5−3.5-fold increased k_D values in comparison with that of the wild-type luciferase. The modest effects of the Phe → Asp mutations on intermediate II dark decay rate suggest that these four Phe residues are primarily involved in maintaining a hydrophobic active site environment rather than directly shielding the flavin C-4a site of the intermediate II. The presence of dodecanol stabilized all intermediate II species from the wild-type enzyme and the four luciferase mutants, with II from αF46D and αF117D being 2−3-fold more stable than the wild-type II. Lowering the temperature to 4 °C in the absence of dodecanol stabilized all intermediate II species but to different degrees, with k_D values of the four mutant intermediate II species ranging from 2-fold smaller to 2-fold larger than that of the wild-type II. At 4 °C, dodecanol had greater stabilizing effects on the mutant intermediate II species, giving rise to more stable intermediate II for the four luciferase mutants than that of the wild-type luciferase.

Stopped-Flow Measurement of Luciferase-Catalyzed $FMNH_2$ Oxidation. The $FMNH_2$ oxidation catalyzed by various luciferase species was examined by stopped-flow spectroscopy in order to determine the effects of luciferase mutations on the yields of intermediate II. In comparison with $FMNH_2$, FMN has markedly increased absorption in the range of 360−510 nm. When $FMNH_2$ is oxidized to FMN without involving the intermediate II, the absorbance increases monitored at any chosen wavelength from 360 to 510 nm would follow the same time course. An example of such a process is the autoxidation of $FMNH_2$, for which the time course of normalized absorbance increases ($\Delta A/\Delta A_\infty$) at 382 nm was indeed identical to that at 445 nm as shown in Figure 1A. In contrast, the luciferase-catalyzed oxidation of bound $FMNH_2$ involves first a rapid formation of intermediate II and then a slow decay of II to FMN (*16*, *18*). Moreover, this overall process is characterized by different time courses of absorbance changes at 338 and 445 nm. The absorption spectrum of intermediate II is distinct from that of $FMNH_2$ and FMN and is characterized by a peak at 372 nm. Moreover, intermediate II shares with FMN an isosbestic point at 382 nm with an extinction coefficient twice of that for the bound $FMNH_2$ (*18*). Therefore, the formation of II from $FMNH_2$ is coupled to a rapid and marked increase of A_{338}, but no further change in A_{338} is associated with the decay of II to FMN. At 445 nm, intermediate II has a slightly

Table 2: Comparison of Wild-Type with Mutant Luciferases with Respect to Quantum Yield, Intermediate II Dark Decay, Yield of Intermediate II, and Aldehyde Consumption

enzyme	$\phi_\circ/\phi_{\circ-WT}$	k_D[a] (min^{-1}) at 23 °C		k_D[a] (min^{-1}) at 4 °C		yield of II[b] (%)	decanal oxidation[c] (%)
		− dodecanol	+ dodecanol	− dodecanol	+ dodecanol		
wild-type	1	2.1	0.12	0.08	0.015	92	84 ± 1
αF46D	8.4×10^{-3}	3.3	0.04	0.10	0.005	30	30 ± 2
αF49D	5.2×10^{-4}	3.0	0.61	0.04	0.006	45	6 ± 2
αF114D	5.1×10^{-2}	7.2	0.22	0.13	0.001	39	14 ± 8
αF117D	7.7×10^{-4}	6.7	0.05	0.15	0.006	<3	6 ± 2

[a] Apparent first-order rate constant for the dark decay of intermediate II in the absence of aldehyde. [b] Based on stopped-flow data obtained at 23 °C as shown in Figure 1. The usual errors were ±2−3%. [c] Determined at 23 °C in triplets.

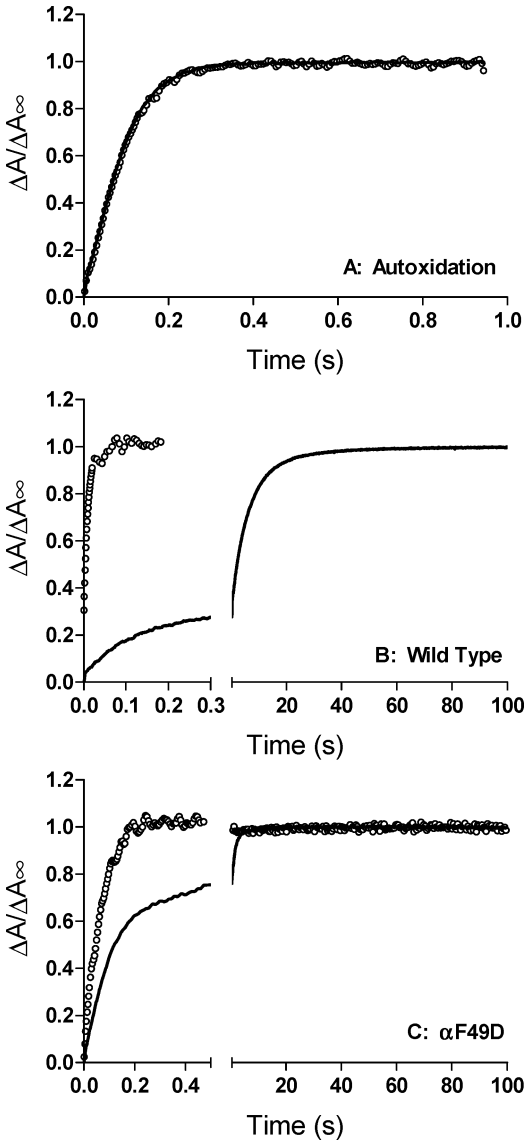

FIGURE 1: Comparison of time course of $FMNH_2$ autoxidation and the oxidations catalyzed by wild-type luciferase and αF49D. An anaerobic 50 mM phosphate buffer, pH 7.0, containing 50 μM $FMNH_2$ and 10 mM EDTA was mixed with an equal volume of an air-saturated 50 mM phosphate buffer, pH 7.0, containing no luciferase (A), 135 μM of the wild-type luciferase (B), or αF49D (C) by using an Olis stopped-flow spectrophotometer. The oxidation of $FMNH_2$ was followed by monitoring the changes in ΔA_{382} (open circles) and ΔA_{445} (solid line). For direct graphic comparisons of the time courses of ΔA_{382} with that of ΔA_{445}, all absorbance changes at a given wavelength were expressed as fractions of the maximal change at the same wavelength as $\Delta A/\Delta A_\infty$, where ΔA and ΔA_∞ are the increases in absorbance from time zero to, respectively, a given time after the mixing and the completion of the reaction.

higher absorbance than $FMNH_2$ and both are much weaker in absorption than FMN. Hence, the conversion of $FMNH_2$ to II is typified by a rapid but small increase of A_{445} with the subsequent decay of II to FMN associated with a slow but sizable increase of A_{445}. As a positive control, the wild-type luciferase-catalyzed oxidation of $FMNH_2$ was monitored by stopped-flow spectroscopy and results are shown in Figure 1B. The formation of II was indicated by a fast rise in A_{382} with little increases of A_{445} within the initial 0.1 s. After the first 0.1 s, no further increases of A_{382} were detected but a large and slow increase of A_{445} was observed for the decay of II to FMN. A comparison of the observed increase of A_{445} when the maximal increase of A_{382} was achieved with the maximal increase of A_{445} upon the completion of the oxidation reaction allows the determination of the percentage yield of intermediate II. On the basis of results shown in Figure 1B, 92% yield of II was detected for the wild-type luciferase (Table 2). Figure 1C shows the results for the αF49D-catalyzed oxidation of $FMNH_2$. A fast increase in A_{382} was observed for the first 0.2 s. During this initial 0.2 s, a partial but sizable increase in A_{445} was also detected. Subsequently, no further changes in A_{382} were observed, but the A_{445} continued with a slow increase until completion of the reaction. The yield of II in the αF49D-catalyzed oxidation of $FMNH_2$ was similarly calculated to be 45% (Table 2). The αF46D-, αF114D-, and αF117D-catalyzed oxidation of $FMNH_2$ were similarly monitored by stopped-flow spectroscopy (results not shown), allowing the determination of 30, 39, and <3% as their respective yields of II (Table 2).

Aldehyde Consumption. The monooxygenation of aldehyde to the corresponding carboxylic acid is coupled to the formation of the light emitting intermediate IV* in the luciferase-catalyzed bioluminescence reaction (*19*). The capabilities of the four Phe → Asp luciferase variants to convert aldehyde to carboxylic acid were examined and compared with that of the wild-type luciferase (Table 2). Using a limited amount of decanal (0.5 μM) and excess luciferase (10 μM) and $FMNH_2$ (25 μM), about 84 ± 1% of decanal was consumed by the wild-type luciferase. The abilities to oxidize decanal by luciferase variants were similarly determined using $FMNH_2$ at 25 μM for αF49D and αF114D, 60 μM for αF117D, and 175 μM for αF46D due to differences in their K_{mF} values. All luciferase mutants showed decreased abilities to oxidize aldehyde, ranging from 30 ± 2 and 14 ± 8% decanal oxidation by αF46D and αF114D, respectively, to a low level of 6 ± 2% for αF49D and αF117D (Table 2).

DISCUSSION

A conserved αF261 is located in a mobile loop next to the opening of the proposed luciferase active site pocket. Our site-directed mutagenesis study of this residue demonstrated that the hydrophobic nature of αF261 is critical to the bioluminescence activity of luciferase. (*12*). We also recently reported that the microenvironment of luciferase active site is suitable for a marked enhancement of the fluorescence quantum yield of 5-decyl-4a-hydroxy-4a,5-dihydroFMN (a model for the proposed luciferase excited emitter IV* shown in Scheme 1) to a level of 50% of the overall quantum yield $\phi_\circ$ (*13*). These reports suggest that the hydrophobicity of the luciferase active site is an important determinant for the bioluminescence efficiency of luciferase. This work was initiated to first test such a working hypothesis by the identification of additional essential phenylalanine residues near the proposed active site pocket and the characterization of the effects of the mutation of these residues to probe their potential functional roles. Second, since the atomic structure of luciferase active site has not been determined, this work was carried out to further map the luciferase active site by mutations of strategically selected residues. To these ends, six conserved phenylalanine residues near the proposed active site pocket (namely αF6, αF46, αF49, αF114, αF117, and αF327) were first each mutated to an alanine. The initial screening of the in vivo biolumi-

nescence of cells harboring these mutated luciferase genes allowed us to focus on αF46, αF49, αF114, and αF117 for additional mutations and detailed characterizations of the mutated luciferases.

In addition to the mutation to an Ala, αF46, αF49, αF114, and αF117 were also each mutated to Asp, Ser, and Tyr. From the results shown in Table 1, no marked changes in K_{mA} were detected for any of these 16 luciferase variants and very little changes in K_{mF} resulted from the four mutations of αF49 or αF114. However, for αF46 and αF117, marked increases in K_{mF} were found for mutation to the anionic Asp. Such an adverse effect on K_{mF} was substantially lessened by mutations to the neutral Ser and Ala and even slightly overcompensated by mutation to the hydrophobic Tyr. These findings suggest that the hydrophobic nature of αF46 and αF117 contributes to the binding of the $FMNH_2$ substrate.

When the hydrophobic Phe was mutated to an anionic Asp, αF46D, αF49D, αF114D, and αF117D showed markedly reduced V_{max} and V_{max}/K_{mF}, ranging from 3 to 5 orders of magnitude lower than those of the native luciferase. Importantly, progressive and substantial recoveries of V_{max} and V_{max}/K_{mF} were achieved when the anionic Asp was replaced by the neutral Ser or Ala and, further, by the hydrophobic Tyr for mutation. It should be noted that the replacement of Asp by Tyr for mutation resulted in all cases in enhancements of V_{max} and V_{max}/K_{mF} by 2−3 orders of magnitude. These results clearly indicate that the hydrophobicity of the conserved αF46, αF49, αF114, and αF117 was critical to the expression of the luciferase activity.

While V_{max} is the maximal rate of quantum production (in q/s) of luciferase (measured as the maximal peak intensity of bioluminescence at saturating substrates), the overall quantum yield ($\phi_\circ$) of the luminescence reaction is based on the total quantum output. On the basis of Scheme 1, $\phi_\circ$ can be expressed by the following relationship:

$$\phi_\circ = Y_{II}Y_{III}Y_{IV^*}\phi_{IV^*} \quad (1)$$

where each Y is the yield of an intermediate (defined by the subscript) and ϕ_{IV^*} is the emission quantum yield of the excited emitter IV*. Reductions in luciferase $\phi_\circ$ can be a consequence of diminished values of any one or any combination of the factors indicated in eq 1. To further identify the causes for the drastically reduced abilities to emit light, the Phe → Asp mutants of αF46, αF49, αF114, and αF117 were subjected to additional characterizations with respect to yields of luciferase intermediates and ϕ_{IV^*}.

The major factor(s) that led to the drastically diminished $\phi_\circ$ of the four mutants shown in Table 2 can be apparently grouped into two types. The first group consists of αF46D, αF49D, and αF117D for which their much reduced $\phi_\circ$ values were a consequence of diminished Y_{II}, $Y_{III}Y_{IV^*}$, and ϕ_{IV^*}. The yields of intermediate II by the native and mutated luciferases can be determined from the stopped-flow experiments (Figure 1). A 30% yield of intermediate II was determined from stopped-flow data for αF46D using 25 μM $FMNH_2$ (after mixing), which is significantly lower than the K_{mF}. Under optimal conditions, the yield of II by αF46D from luciferase-bound $FMNH_2$ should be >30%. The yields of intermediate III and IV* were not individually determined in this work. However, our available results provide estimates of these yields. The yield of III is determined by a competition between the dark decay of II (k_D) with the rate of III formation from II and aldehyde. While the latter rate was not determined, the k_D values for αF46D were ≤3-fold different from that of the wild-type luciferase at 23 or 4 °C in the absence or presence of dodecanol as a stabilizing agent. These results suggest that the yield of III by αF46D was unlikely to be drastically lower than that of the wild-type enzyme. Moreover, the formation of the excited emitter IV* is coupled to the oxidation of aldehyde substrate to carboxylic acid (*19*). Therefore, the percentage oxidation of decanal using excess luciferase and $FMNH_2$ (i.e., 30 ± 2% in this case of αF46D) provides an estimate of the combined $Y_{III}Y_{IV^*}$ term in eq 1. The Y_{II} at ≥30% together with the measured $\phi_\circ/\phi_{\circ-WT}$ at 8.4×10^{-3} and decanal oxidation ($\approx Y_{III}Y_{IV^*}$) at 30% allowed an estimate of the ϕ_{IV^*} of αF46D to be about 1 order of magnitude lower than that of the wild-type luciferase. Therefore, the 3 orders of magnitude reduction in $\phi_\circ$ for αF46D was a result of the mutational effects on all three parameters of Y_{II}, $Y_{III}Y_{IV^*}$, and ϕ_{IV^*}. By similar analyses of results shown in Table 2, the approximated ϕ_{IV^*} value of αF114D was found resembling that of the native luciferase, whereas those of αF117D and αF49D were reduced by 1 and 2 orders of magnitude, respectively. Therefore, αF49D and αF117D were similar to αF46D in that their marked reduced $\phi_\circ$ values were consequences of compromised Y_{II}, $Y_{III}Y_{IV^*}$, and ϕ_{IV^*}. The αF114D was an apparent exception from the first group. Among the four Phe → Asp mutants, αF114D had the least pronounced (i.e., at 20-fold) reduction in $\phi_\circ$, which can be essentially accounted for by decreased yield of Y_{II} and decanal oxidation without having to resort to significant changes in its ϕ_{IV^*}. As already mentioned, αF114D also differed from the wild-type luciferase and αF46D, αF49D, and αF117D variants in exhibiting a double-exponential decay time course in the nonturnover bioluminescence reaction. The molecular basis for such a change of light decay kinetics remains unclear. This uncertainty, however, does not directly impact on conclusions made in this or our earlier reports.

Although with differences in details, the hydrophobic nature of αF46, αF49, αF114, and αF117 was shown to be critical to the bioluminescence activity of luciferase through their essentialities to Y_{II}, $Y_{III}Y_{IV^*}$ and, with the exception of αF114D, ϕ_{IV^*}. These findings are quite consistent with literature information. As has been revealed from flavin models, the dark decay of intermediate II can be effectively retarded in a more hydrophobic environment (*20*). Also, the binding of hydrophobic long-chain alcohols to luciferase remarkably enhanced the stability of intermediate II (*16*). Therefore, a hydrophobic microenvironment of the luciferase active site may contribute to reduced dark decay of intermediate II, enhanced yield of intermediate III, and, possibly, a better yield of IV* by enhanced aldehyde binding. We have recently shown that the fluorescence quantum yield of a IV* model compound 5-decyl-4a,5-dihydroriboflavin-5′-phosphate can be enhanced by at least 3 orders of magnitude by binding to luciferase (*13*). On the basis of previous studies of the medium hydrophobicity on fluorescence intensities of various flavins (*21, 22*), such a marked fluorescence enhancement of 5-decyl-4a,5-dihydroriboflavin-5′-phosphate by luciferase binding is, at least in part, a consequence of the hydrophobic environment of the luciferase active site.

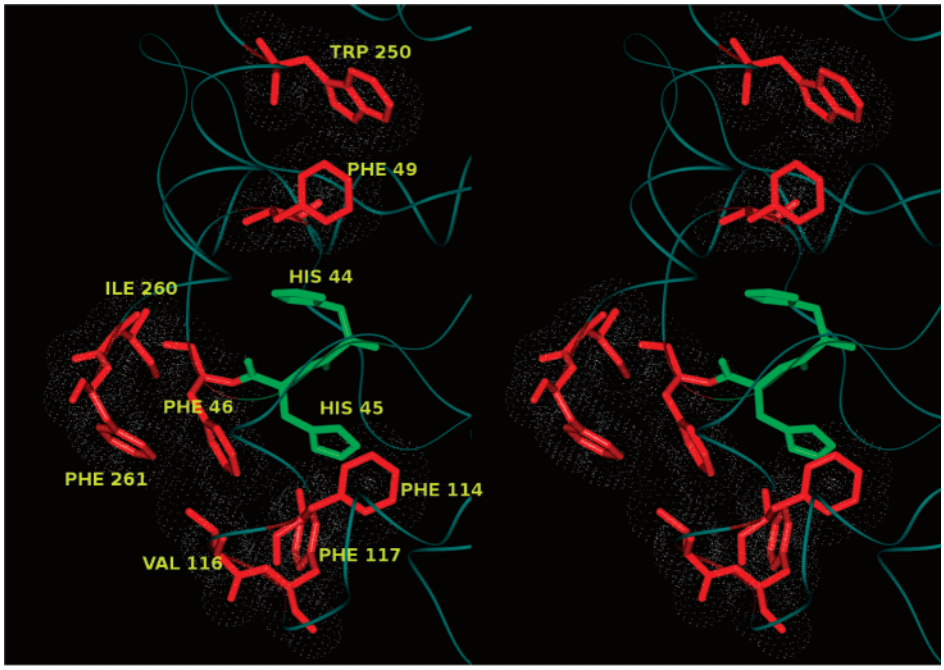

FIGURE 2: Contributions of αF46, αF49, αF114, and αF117 to a hydrophobic cluster and their locations within the proposed luciferase active site. The light blue wire frame represents the backbone of the α subunit. The essential αH44 and αH45 (both in green) are surrounded by hydrophobic residues αF46, αF49, αF114, αV116, αF117, αW250, αI260, and αF261 (all in red). αF261 and αI260 are at one end of a mobile loop which, as a whole, has been proposed to function as a gate for the active site during catalysis. For additional shielding of the active site from aqueous solvent, residue αF46 packs well with residues αV116, αF117, and αF114 to form a tight, hydrophobic barrier near αH45, whereas αF49 and the nearby αW250 form another hydrophobic cluster near αH44. αF49 and the neighboring αH44 were important to aldehyde oxidation, whereas αF117 and αH45 were close to each other and were both essential to the formation of intermediate II. van der Waals surfaces are represented by white dots for all the red color hydrophobic side chains depicted in this figure.

The originally proposed general location of the luciferase active site pocket (*4*, *5*) and the essential role of αR107 in $FMNH_2$ phosphate binding (*8*) form a basis for a computational model of the luciferase active site (*9*). Essential residues revealed by earlier and the present site-directed mutagenesis studies provide a test to the proposed active site and more definitively depict the makeup of the active site of luciferase as shown in Figure 2. αH44 and αH45 have been shown to be critical to luciferase activity (*14*) with the former as a catalytic base participating at a step after the formation of intermediate II (*23*) and the latter essential to the formation of intermediate II (*24*). These two essential histidine residues are sandwiched between αF49 and αF117 with all four residues aligned almost along a linear path. It is interesting to note that αF49 is next to αH44 and is similarly important to the oxidation of aldehyde substrate, whereas αF117 is next to αH45 and both are essential to a high yield of intermediate II (Table 2). In the orientation as shown in Figure 2, the opening of the luciferase active site is facing the 10 o'clock direction. αH44 and αH45 are shielded from a direct exposure to aqueous medium by two hydrophobic clusters. One hydrophobic cluster comprising αF49 and αW250 is next to αH44. In this connection, αW250 has been shown to be important to the binding of $FMNH_2$ and aldehyde (*25*). The other hydrophobic barrier is near αH45 and consists of residues αF114, αF117, αV116, αF46, αF261, and αI260. Moreover, αF261 and αI260 are at one end of a mobile loop which, as a whole, has been proposed to function as a gate to shield the active site-bound intermediates during catalysis (*12*, *26*). In all, a number of hydrophobic residues within the active site and the mobile loop itself provide a network to ensure a generally hydrophobic environment of the luciferase active site. Of these essential hydrophobic residues, the functional roles of αF46, αF49, αF114, and αF117 were revealed in this work.

ACKNOWLEDGMENT

We would like to thank Dr. Thomas Russell for his technical assistance in stopped-flow spectroscope and Jerry Osagie Ebalunode for his help in displaying the stereoview of the protein structure.

REFERENCES

1. Hastings, J. W., Potrikus, C. J., Gupta, S. C., Kurfürst, M., and Makemson, J. C. (1985) Biochemistry and physiology of bioluminescent bacteria, *Adv. Microb. Physiol. 26*, 235−291.
2. Tu, S.-C. (2003) Bacterial bioluminescence: biochemistry, in *CRC Handbook of Organic Photochemistry and Photobiology* (Horspool, W. M., and Lenci, F., Eds.) p 136.131−136.117, CRC Press, Boca Raton, FL.
3. Baldwin, T. O., Christopher, J. A., Raushel, F. M., Sinclair, J. F., Ziegler, M. M., Fisher, A. J., and Rayment, I. (1995) Structure of bacterial luciferase, *Curr. Opin. Struct. Biol. 5*, 798−809.
4. Fisher, A. J., Raushel, F. M., Baldwin, T. O., and Rayment, I. (1995) Three-dimensional structure of bacterial luciferase from *Vibrio harveyi* at 2.4 Å resolution, *Biochemistry 34*, 6581−6586.
5. Fisher, A. J., Thompson, T. B., Thoden, J. B., Baldwin, T. O., and Rayment, I. (1996) The 1.5-Å resolution crystal structure of bacterial luciferase in low salt conditions, *J. Biol. Chem. 271*, 21956−21968.
6. Becvar, J. E., and Hastings, J. W. (1975) Bacterial luciferase requires one reduced flavin for light emission, *Proc. Natl. Acad. Sci. U.S.A. 72*, 3374−3376.
7. Lei, B., Cho, K. W., and Tu, S.-C. (1994) Mechanism of aldehyde inhibition of *Vibrio harveyi* luciferase. Identification of two aldehyde sites and relationship between aldehyde and flavin binding, *J. Biol. Chem. 269*, 5612−5618.
8. Moore, C., Lei, B., and Tu, S. C. (1999) Relationship between the conserved alpha subunit arginine 107 and effects of phosphate on the activity and stability of *Vibrio harveyi* luciferase, *Arch. Biochem. Biophys. 370*, 45−50.

9. Lin, L. Y., Sulea, T., Szittner, R., Vassilyev, V., Purisima, E. O., and Meighen, E. A. (2001) Modeling of the bacterial luciferase-flavin mononucleotide complex combining flexible docking with structure−activity data, *Protein Sci. 10*, 1563−1571.
10. Lin, L. Y., Sulea, T., Szittner, R., Kor, C., Purisima, E. O., and Meighen, E. A. (2002) Implications of the reactive thiol and the proximal non-proline cis-peptide bond in the structure and function of *Vibrio harveyi* luciferase, *Biochemistry 41*, 9938−9945.
11. Lin, L. Y., Szittner, R., Friedman, R., and Meighen, E. A. (2004) Changes in the kinetics and emission spectrum on mutation of the chromophore-binding platform in *Vibrio harveyi* luciferase, *Biochemistry 43*, 3183−3194.
12. Low, J. C., and Tu, S.-C. (2002) Functional roles of conserved residues in the unstructured loop of *Vibrio harveyi* bacterial luciferase, *Biochemistry 41*, 1724−1731.
13. Lei, B., Ding, Q., and Tu, S.-C. (2004) Identity of the emitter in the bacterial luciferase luminescence reaction: binding and fluorescence quantum yield studies of 5-decyl-4a-hydroxy-4a,5-dihydroriboflavin-5′-phosphate as a model, *Biochemistry 43*, 15975−15982.
14. Xin, X., Xi, L., and Tu, S. C. (1991) Functional consequences of site-directed mutation of conserved histidyl residues of the bacterial luciferase alpha subunit, *Biochemistry 30*, 11255−11262.
15. Lei, B. F., and Becvar, J. E. (1991) A new reducing agent of flavins and its application to the assay of bacterial luciferase, *Photochem. Photobiol. 54*, 473−476.
16. Tu, S.-C. (1979) Isolation and properties of bacterial luciferase-oxygenated flavin intermediate complexed with long-chain alcohols, *Biochemistry 18*, 5940−5945.
17. Meighen, E. A. (1991) Molecular biology of bacterial bioluminescence, *Microbiol. Rev. 55*, 123−142.
18. Hastings, J. W., Balny, C., LePeuch, C., and Douzou, P. (1973) Spectral properties of an oxygenated luciferase-flavin intermediate isolated by low-temperature chromatography, *Proc. Natl. Acad. Sci. U.S.A. 70*, 3468−3472.
19. Dunn, D. K., Michaliszyn, G. A., Bogacki, I. G., and Meighen, E. A. (1973) Conversion of aldehyde to acid in the bacterial bioluminescent reaction, *Biochemistry 12*, 4911−4918.
20. Kemal, C., and Bruice, T. C. (1976) Simple synthesis of a 4a-hydroperoxy adduct of a 1,5-dihydroflavine: preliminary studies of a model for bacterial luciferase, *Proc. Natl. Acad. Sci. U.S.A. 73*, 995−999.
21. Ghisla, S., Massey, V., Lhoste, J.-M., and Mayhew, S. G. (1974) Fluorescence and optical characteristics of reduced flavins and flavoproteins, *Biochemistry 14*, 589−597.
22. Kaaret, T. W., and Bruice, T. C. (1990) Electrochemical luminescence with N(5)-ethyl-4a-hydroxy-3-methyl-4a,5-dihydrolumiflavin. The mechanism of bacterial luciferase, *Photochem. Photobiol. 51*, 629−633.
23. Huang, S., and Tu, S. C. (1997) Identification and characterization of a catalytic base in bacterial luciferase by chemical rescue of a dark mutant, *Biochemistry 36*, 14609−14615.
24. Li, H., Ortego, B. C., Maillard, K. I., Willson, R. C., and Tu, S. C. (1999) Effects of mutations of the alpha His45 residue of *Vibrio harveyi* luciferase on the yield and reactivity of the flavin peroxide intermediate, *Biochemistry 38*, 4409−4415.
25. Li, Z., and Meighen, E. A. (1995) Tryptophan 250 on the α subunit plays an important role in flavin and aldehyde binding to bacterial luciferase. Effects of W→Y mutations on catalytic function, *Biochemistry 34*, 15084−15090.
26. Sparks, J. M., and Baldwin, T. O. (2001) Functional implications of the unstructured loop in the $(\beta/\alpha)_8$ barrel structure of the bacterial luciferase α subunit, *Biochemistry 40*, 15436−15443.

BI050935Y